

Electronic Supplementary Information
for

Quasi Single-crystalline Transformation of Porous Frameworks Accompanied with Interlayer Rearrangements of Hydrogen Bonds

Haruka Kubo, Ryusei Oketani, Ichiro Hisaki*

*Division of Chemistry, Graduate School of Engineering Science, Osaka University. 1-3
Machikaneyama, Toyonaka, Osaka 560-8531, Japan*

Contents.

1. General

2. Synthesis of compounds

Scheme S1. Synthesis of **BrPQ**.

3. Thermal analysis

Fig. S1 Thermal gravimetric and differential thermal analyses.

4. Crystallography

Table S1. Crystal data of **BrPQ-1**, **BrPQ-2**, **BrPQ-2a**, and **BrPQ-3a**.

Fig. S2 Morphology of single crystals of **BrPQ-1** before and after heating at 120 °C.

Fig. S3 Two kinds of intermolecular hydrogen bonded dimer of the carboxy groups observed in **BrPQ-1**.

Fig. S4 Crystal structures drawn by anisotropic displacement ellipsoids with 50% probability.

Fig. S5 Crystal structure of **BrPQ-2a**

Fig. S6 Overlay plot of crystal structures **BrPQ-2a** and **BrPQ-3a**.

Fig. S7 ¹H NMR spectra of **BrPQ-2a** and **BrPQ-3a** dissolved in DMSO-*d*₆.

5. Structural changes of BrPQ-1 at room temperature

Fig. S8 Time dependent PXRD pattern changes of **BrPQ-1** at room temperature.

6. Gas sorption experiments

Fig. S9 N₂ and CO₂ sorption isotherms of **BrPQ-2a** at 77 K and 195 K, respectively.

7. Stability of BrPQ-2a in polar solvents

Fig. S10 PXRD patterns of **BrPQ-2a** (a) simulated from SXRD data, (b) before immersed in polar solvents, (c) after immersed in hot water (100 °C) for 5 h, and (d) after immersed in hot EtOH (70 °C) for 5 h.

8. NMR spectra

Fig. S11 ¹H NMR (400 MHz, CDCl₃) spectrum of a mixture of **4** and **4'**.

Fig. S12 ¹³C NMR (100 MHz, CDCl₃) and distortionless enhancement of polarization transfer (DEPT) spectra of a mixture of **4** and **4'**.

Fig. S13 Selected spectra of the magnified aromatic region in Fig. S8.

Fig. S14 ^1H -detected multiple quantum coherence (HMQC) spectrum of a mixture of **4** and **4'**.

Fig. S15 ^1H NMR (400 MHz, $\text{DMSO-}d_6$) spectrum of a mixture of **BrPQ** and **Br(H)PQ**.

Fig. S16 ^{13}C NMR (100 MHz, $\text{DMSO-}d_6$) spectrum of a mixture of **BrPQ** and **Br(H)PQ**.

9. References

1. General

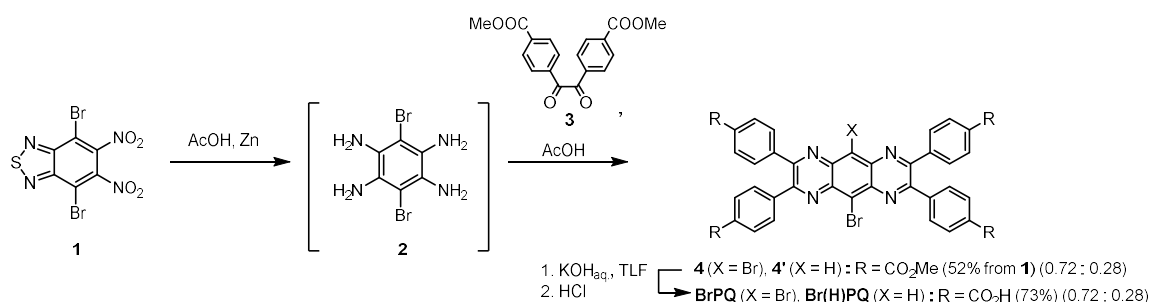
All reagents and solvents were used as received from commercial suppliers. ^1H and ^{13}C NMR spectra were measured on a Bruker AV400M (400 MHz) spectrometer. Residual proton and carbon of deuterated solvents were used as internal standards for the measurements: $\delta = 7.26$ ppm (CDCl_3), $\delta = 2.50$ ppm ($\text{DMSO-}d_6$), $\delta = 5.50$ ppm ($\text{NMP-}d_9$) for ^1H NMR, $\delta = 77.00$ ppm (CDCl_3), $\delta = 39.50$ ppm ($\text{DMSO-}d_6$) for ^{13}C NMR. HR-MS analyses were conducted on a JEOL JMS-700 instrument. Thermal gravimetric (TG) analysis was performed on Rigaku TG8120 under an N_2 purge (100 mL/min) at a heating rate of 5 K min^{-1} .

Powder X-ray diffraction (PXRD) data were collected on a Rigaku Ultima-IV (40 kV, 44 mA) or PANalytical XPert PRO X'Celerator using $\text{Cu-K}\alpha$ radiation at room temperature and with a scan rate of $2.0^\circ\text{ min}^{-1}$. Variable temperature PXRD (VT-PXRD) data were collected on same apparatus as PXRD with a temperature control unit. For VT-PXRD, the HOF powders were placed on an aluminum substrate, and the measurements were conducted in atmospheric conditions. The temperature of the sample was increased from room temperature to 360°C with a rate of 1.0°min^{-1} . PXRD scan of each measurement was collected with a difference in the temperature of ca. 5.1°C

Gas sorption experiments were performed for the activated crystalline bulk of **BrPQ-2a** on BELSORP-max (BEL, Japan). The adsorption isotherms of N_2 and CO_2 were corrected at 77K and 195 K, respectively. Brunauer–Emmett–Teller (BET) specific surface area: SA(BET) was based on CO_2 absorption isotherms.

Single crystal X-ray measurement and analysis. Diffraction data of **BrPQ-1**, **BrPQ-2**, **BrPQ-2a**, and **BrPQ-3a** were collected with a two-dimensional X-ray detector (PILATUS 200K/R) equipped on a Rigaku XtaLAB P200 diffractometer by using $\text{Mo-K}\alpha$ radiation monochromated with multilayer mirror ($\lambda = 0.71073\text{ \AA}$). Diffraction Data collection, cell refinement, and data reduction were carried out with CrysAlis PRO.^{S1} SHELXT^{S2} was used for the structure solution of the crystals. These calculations were performed with the observed reflections [$I > 2\sigma(I)$] with the program CrystalStructure crystallographic software.^{S3} Structural refinement was performed by SHELXL.^{S4} All non-hydrogen atoms were refined with anisotropic displacement parameters, and hydrogen atoms were placed in idealized positions and refined as rigid atoms with the relative isotropic displacement parameters. SQUEEZE function equipped in the PLATON program was used to treat severely disordered solvent molecules in voids.^{S5}

2. Synthesis of compounds



Scheme S1. Synthesis of **BrPQ**.

Dibromopyrazinoquinoxaline derivative 4. A suspension of 2,6-dibromo-4,5-dinitrothiadiazole **1**^{S6} (170 mg, 0.443 mmol) and zinc powder (600 mg, 9.94 mmol) in deoxygenated AcOH (6.00 mL) was stirred for 75 min at 75 °C. To the solution was added another zinc powder (422 mg, 6.64 mmol) and the solution mixture was stirred for another 20 min at 75 °C. The solution mixture including the intermediate 3,6-dibromo-1,2,4,5-benzenetetramine **2** was filtered to remove the unreactive zinc powder. To the filtrate was added benzil derivative **3** (209 mg, 0.568 mmol), and the mixture was stirred at 105 °C for another 24 h. After removing CHCl₃ in vacuo, the precipitate was filtered by a filter paper and carefully rinsed with AcOH and EtOH to give a mixture of **4** and **4'** (130 mg, molar ratio of **4** : **4'** = 1 : 0.4) in 52% yield as yellow solid.

4. ¹H NMR (400 MHz, CDCl₃): δ 8.09 (d, *J* = 8.0 Hz, 8H), 7.83 (d, *J* = 8.3 Hz, 8H), 3.96 (s, 12H) ppm. ¹³C NMR (400 MHz, CDCl₃): δ 166.4, 154.4, 141.5, 138.6, 131.6, 130.4, 129.8, 126.2, 52.4 ppm. HR-MS (FAB): calcd. For C₄₂H₂₉Br₂N₄O₈ [M+H]⁺ 875.0352; found: 875.0349.

4'. ¹H NMR (400 MHz, CDCl₃): δ 9.05 (s, 1H), 8.09 (d, *J* = 8.0 Hz, 4H), 8.07 (d, *J* = 8.0 Hz, 4H), 7.79 (d, *J* = 8.3 Hz, 4H), 7.72 (d, *J* = 8.5 Hz, 1H), 3.96 (s, 12H) ppm. HR-MS (FAB): calcd. For C₄₂H₃₂BrN₄O₈ [M+3H]⁺ 799.1404; found: 799.1233.

BrPQ. A mixture of methyl ester derivative **4** and **4'** (33.4 mg, molar ratio of **4** : **4'** = 1 : 0.4) in THF (15.0 mL) and 5% aqueous solution of KOH (2.00 mL) was stirred for 93 h at 55 °C. After removing THF in vacuo, 6M-HCl was added till further precipitate did not form. The precipitate was collected by centrifuge and washed with water and dried to give mixture of **BrPQ** and **Br(H)PQ** (22.8 mg, molar ratio of **BrPQ** : **Br(H)PQ** = 0.72 : 0.28) in 73% yield as a dark solid.

BrPQ. ¹H NMR (400 MHz, DMSO-*d*₆): δ 7.99 (d, *J* = 8.4 Hz, 8H), 7.79 (d, *J* = 8.4 Hz, 8H) ppm. ¹³C NMR (400 MHz, DMSO-*d*₆): δ 167.72, 155.68, 142.26, 139.02, 132.84, 131.25, 130.04, 126.25 ppm. HR-MS (FAB): calcd. For C₃₈H₂₀Br₂N₄O₈ [M] 817.9648; found: 817.9660.

(Br, H)PQ. ¹H NMR (400 MHz, DMSO-*d*₆): δ 9.01 (s, 1H), 7.99 (d, *J* = 8.4 Hz, 4H), 7.97 (d, *J* =

6.8 Hz, 4H), 7.77 (d, $J = 5.2$ Hz, 4H) , 7.73 (d, $J = 8.8$ Hz, 4H) ppm.

3. Thermal analysis

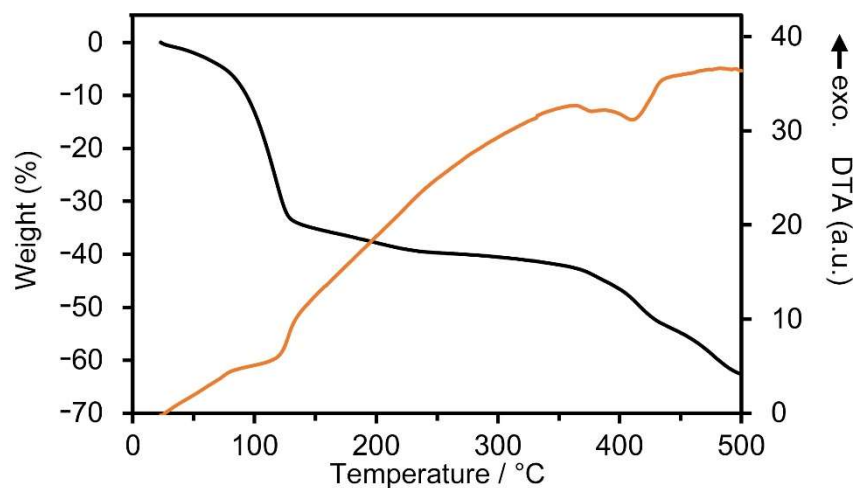


Fig. S1 Thermal gravimetric (black line) and differential thermal (orange line) analyses. TG curve indicates that *o*DCB is included in the framework with a host : guest ratio of 1 : 4 and that 3/4 *o*DCB molecules are removed up to 125 °C, corresponding to weight loss of 33%, and the rest is removed up to 300 °C, corresponding to weight loss of 7.3%. Further weight loss observed at the temperature higher than 370 °C is due to decomposition of the compound.

4. Crystallography

Table S1. Crystal data of **BrPQ-1**, **BrPQ-2**, **BrPQ-2a**, and **BrPQ-3a**

	BrPQ-1	BrPQ-2	BrPQ-2a	BrPQ-3a
Formula	$C_{38}H_{20.28}Br_{1.72}N_4O_8 \cdot 4(C_6H_4Cl_2)$	$C_{38}H_{20.28}Br_{1.72}N_4O_8 \cdot C_6H_4Cl_2$	$C_{38}H_{20.28}Br_{1.72}N_4O_8$	$C_{38}H_{20.28}Br_{1.72}N_4O_8$
Crystal size / mm	0.70 × 0.19 × 0.10	0.15 × 0.05 × 0.05	0.02 × 0.02 × 0.01	0.05 × 0.05 × 0.05
Fw	1386.33	945.28	798.29	798.29
T/K	113	113	113	113
Crystal system	triclinic	triclinic	triclinic	triclinic
Space group	<i>P</i> -1	<i>P</i> -1	<i>P</i> -1	<i>P</i> -1
<i>a</i> / Å	5.48306(15)	5.5503(2)	5.4836(4)	5.584(2)
<i>b</i> / Å	15.3486(4)	11.9493(5)	11.8374(12)	12.305(3)
<i>c</i> / Å	17.9094(5)	15.1638(5)	15.4284(12)	15.827(5)
α / °	79.089(2)	102.503(3)	102.618(8)	103.84(2)
β / °	84.670(2)	91.720(3)	92.409(6)	93.62(3)
γ / °	88.069(2)	92.766(3)	92.015(7)	91.13(3)
<i>V</i> / Å ³	1473.36(7)	979.86(6)	975.42(15)	1053.1(6)
<i>Z</i>	1	1	1	1
GOF	1.071	1.081	0.953	0.916
No of reflns. obs./uniq.	23851/8353	16915/ 5683	13468/ 4621	17280/ 6035
<i>R</i> _{<i>i</i>} [<i>I</i> > 2σ(<i>I</i>)], w <i>R</i> ₂ (all data)	0.031, 0.093	0.054, 0.160	0.080, 0.222	0.106, 0.327
CCDC No.	2088687	2088688	2088689	2088690

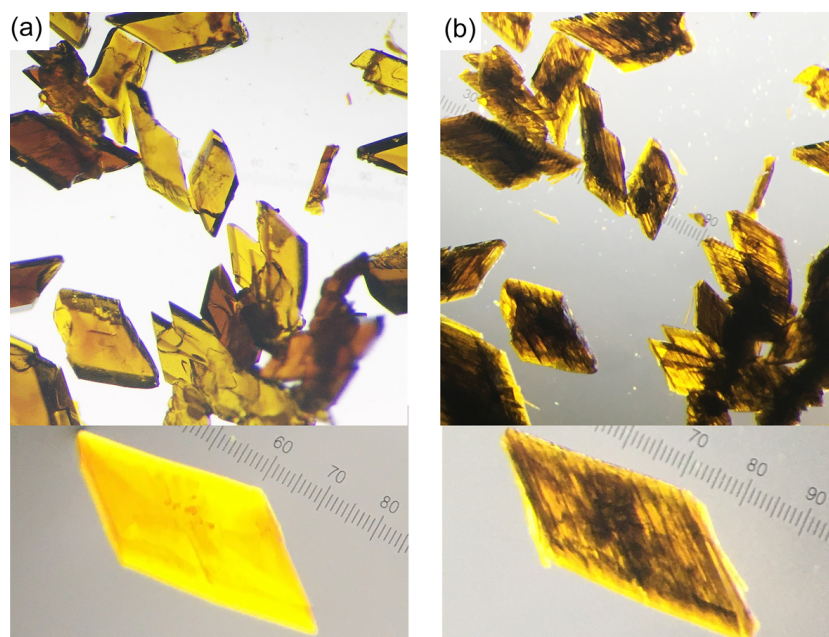


Fig. S2 Morphology of single crystals of **BrPQ-1** before (a) and after heating at 120 °C (b).

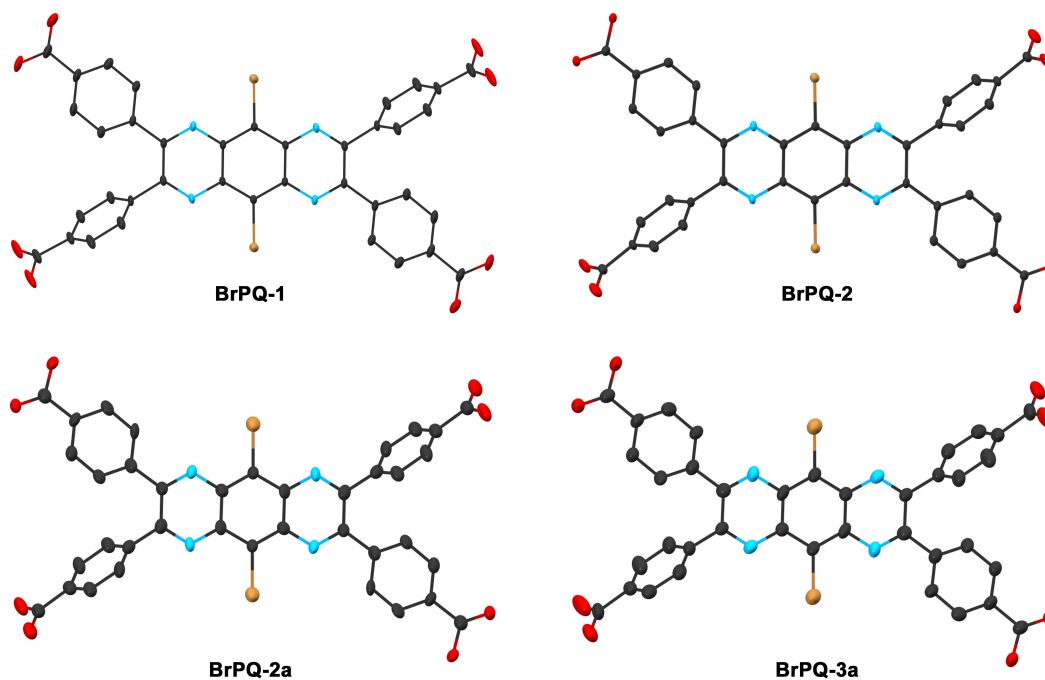


Fig. S3 Crystal structures drawn by anisotropic displacement ellipsoids with 50% probability.

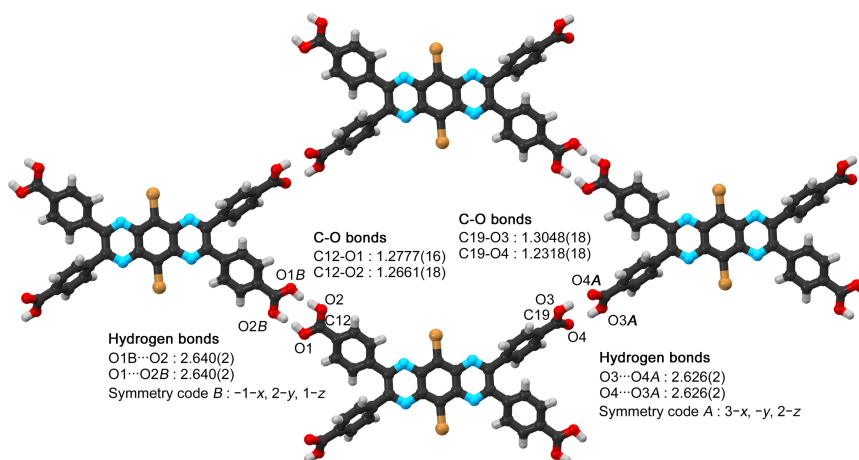


Fig. S4 Two kinds of intermolecular hydrogen bonded dimer of the carboxy groups observed in **BrPQ-1**. In the case of the dimer involving the carboxy group composed of C12, O1, and O2 atoms, the hydrogen atom is disordered in two positions, while in the case of the dimer involving C19, O4, and O3 atoms, the hydrogen atom is localized at O3. These are indicated by the C–O distances of the carboxy group.

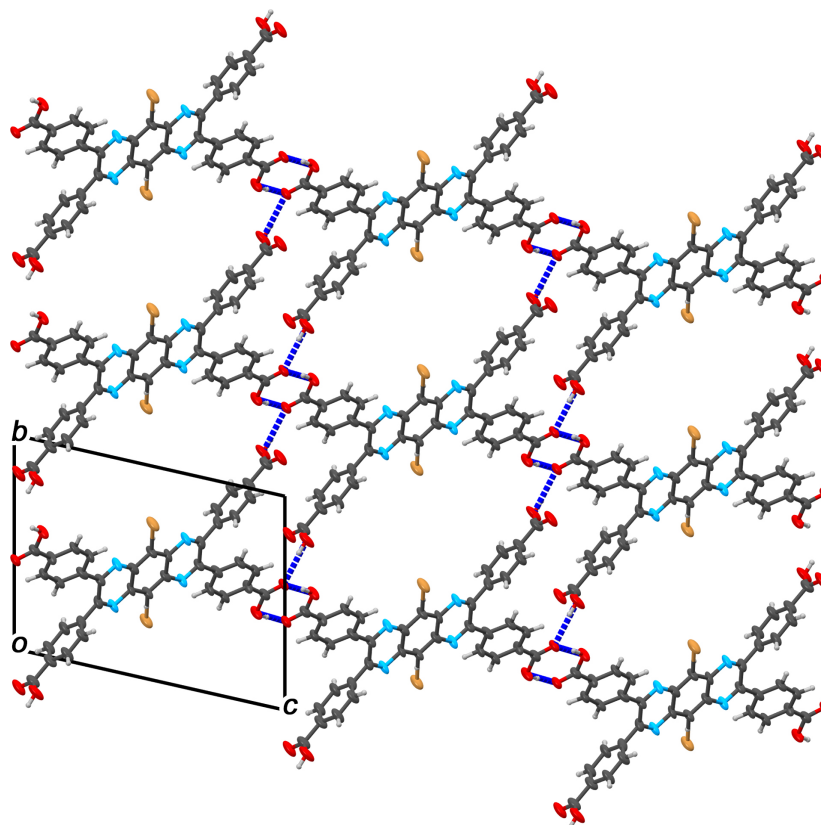


Fig. S5. Crystal structure of **BrBQ-2a**. Atoms except for hydrogen are drawn with anisotropic displacement ellipsoids in 50% probability.

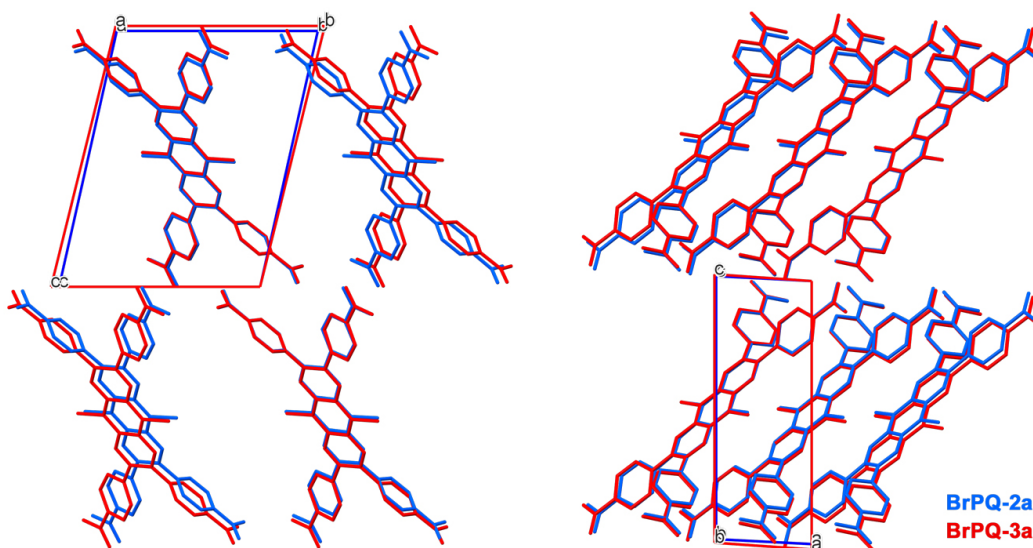


Fig. S6 Overlay plot of crystal structures **BrPQ-2a** and **BrPQ-3a** view from the *a* axis (left) and the *b* axis (right).

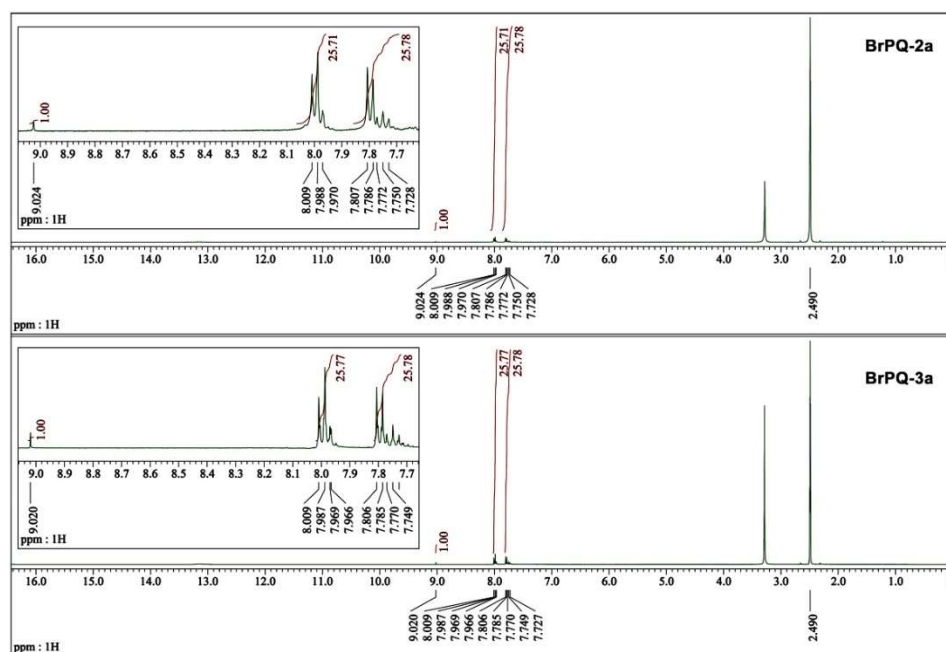


Fig. S7 ¹H NMR spectra of, **BrPQ-2a** and **BrPQ-3a** dissolved in DMSO-*d*₆.

5. Structural changes of BrPQ-1 at room temperature

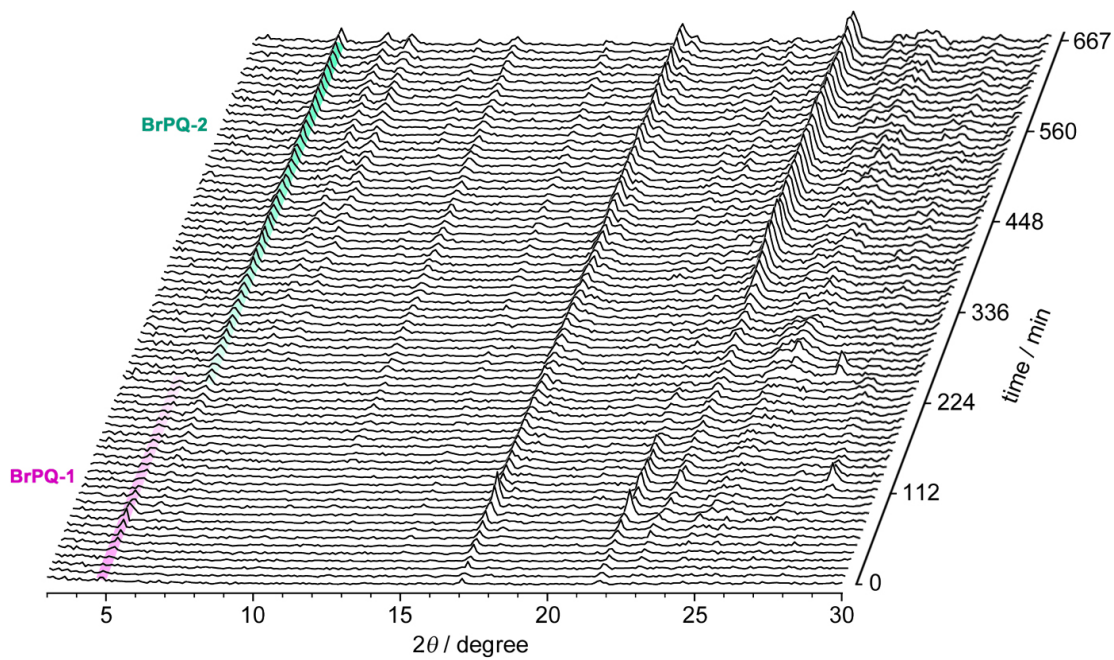


Fig. S8 Time dependent PXRD pattern changes of **BrPQ-1** at room temperature (20 °C).

6. Gas sorption experiments

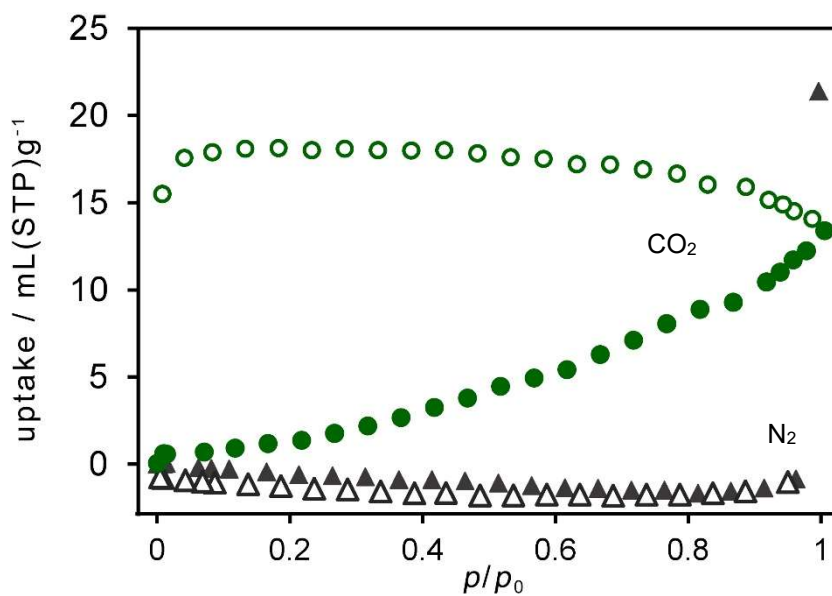


Fig. S9 N₂ (triangle) and CO₂ (circle) sorption isotherms of **BrPQ-2a** at 77 K and 195 K, respectively. Filled symbol: adsorption process. Open symbol: desorption process. **BrPQ-2a** show no uptake of N₂, while gave unusual CO₂ sorption isotherms with significant hysteresis. This indicates that uptake of CO₂ undertakes so slowly because of narrow width of the 1D pores and that strong attractive interactions forms between the pore wall of the framework and molecules of CO₂.

7. Stability of BrPQ-2a in polar solvents

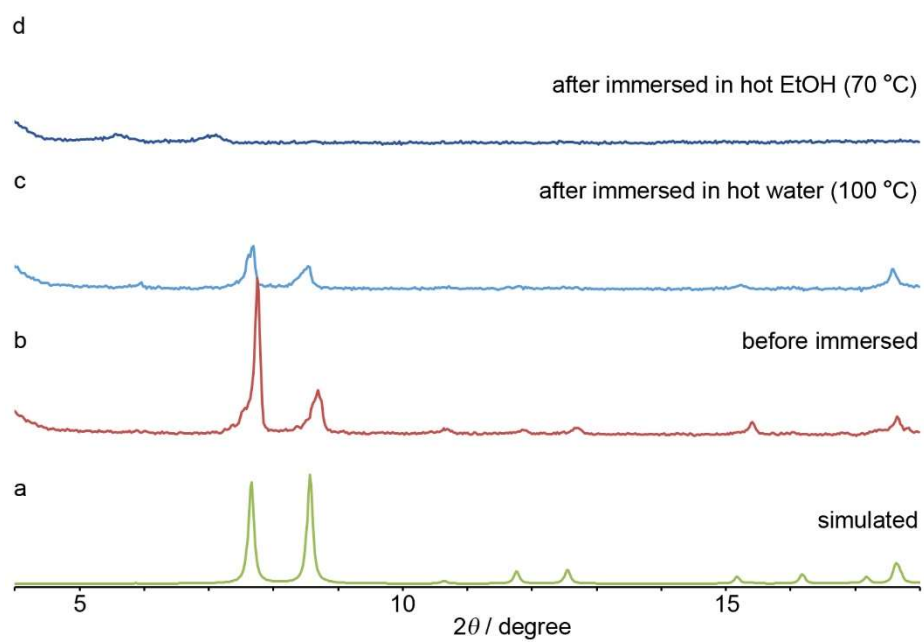


Fig. 10 PXRD patterns of **BrPQ-2a** (a) simulated from SXRD data, (b) before immersed in polar solvents, (c) after immersed in hot water (100 °C) for 5 h, and (d) after immersed in hot EtOH (70 °C) for 5 h. A framework of **BrPQ-2a** was collapsed after immersed in hot EtOH.

8. NMR spectra

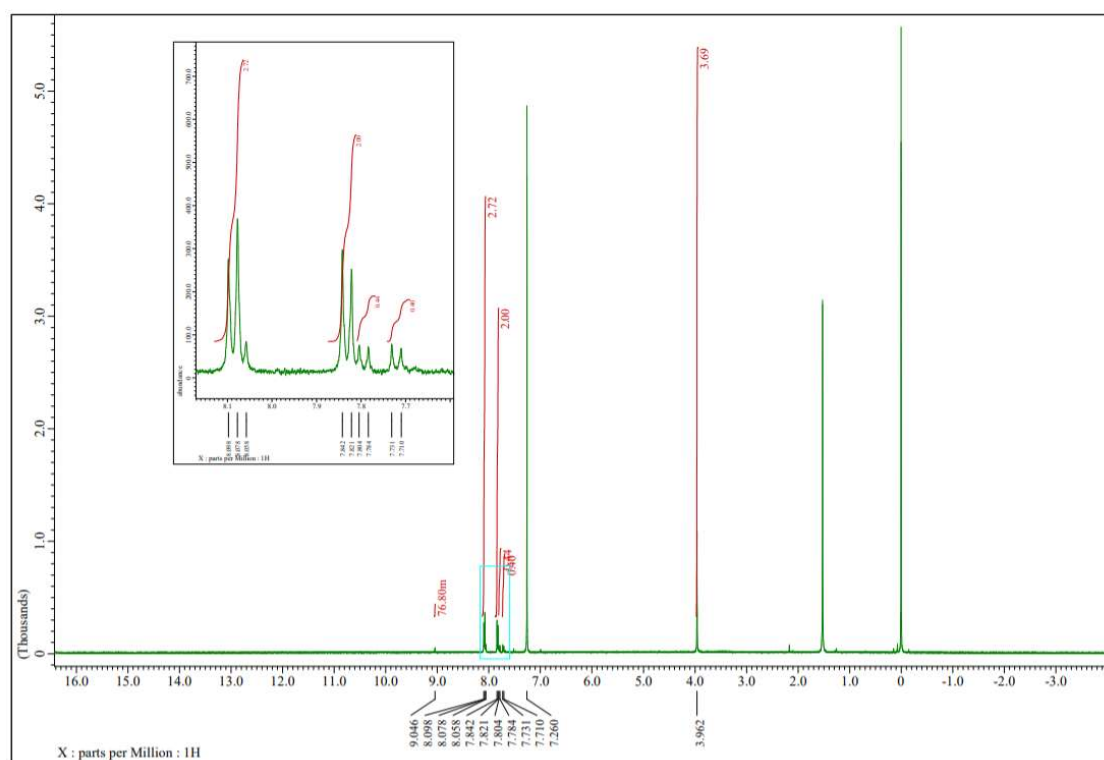


Fig. S11 ^1H NMR (400 MHz, CDCl_3) spectrum of a mixture of **4** and **4'**. A molar ratio of **4** : **4'** is 1 : 0.4.

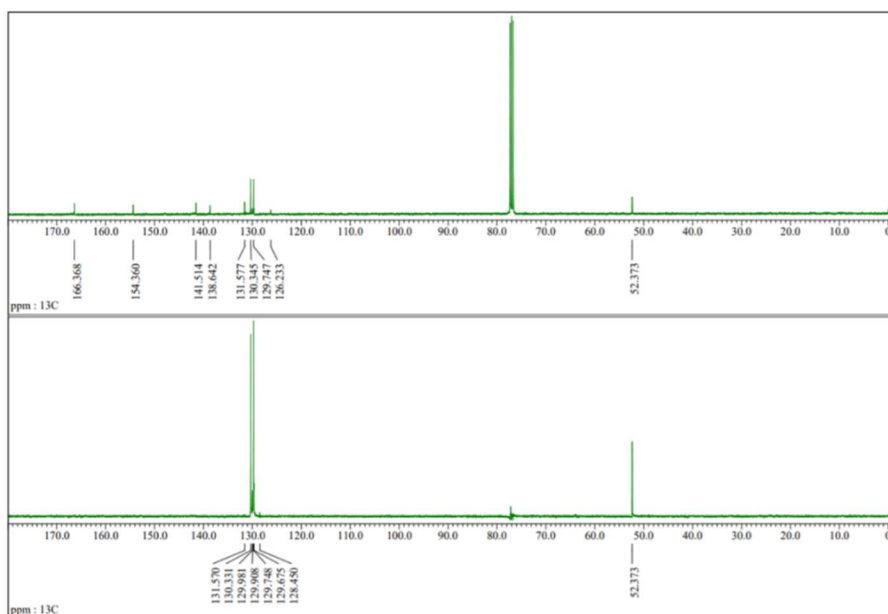


Fig. S12 (Top) ^{13}C NMR (100 MHz, CDCl_3) and (Bottom) DEPT ^{13}C NMR (135°) (100 MHz, CDCl_3) spectra of a mixture of **4** and **4'**. Only Peaks of **4** are picked in the top spectrum and the characteristic peaks ascribable to **4'** are identified by DEPT (135°) [Fig. S8 Bottom] and HMQC NMR spectrum in Fig. S9.

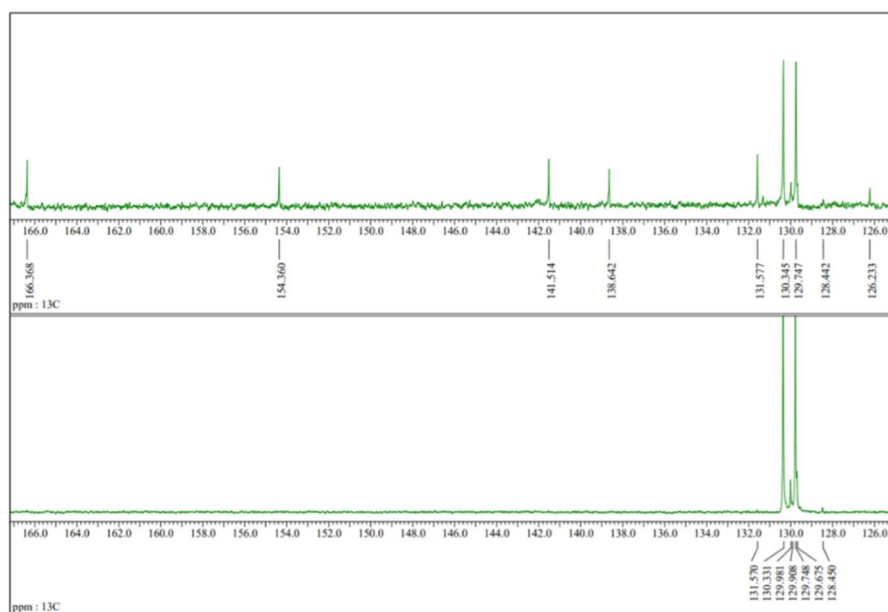


Fig. S13 Selected spectra of the magnified aromatic region in Fig. S9.

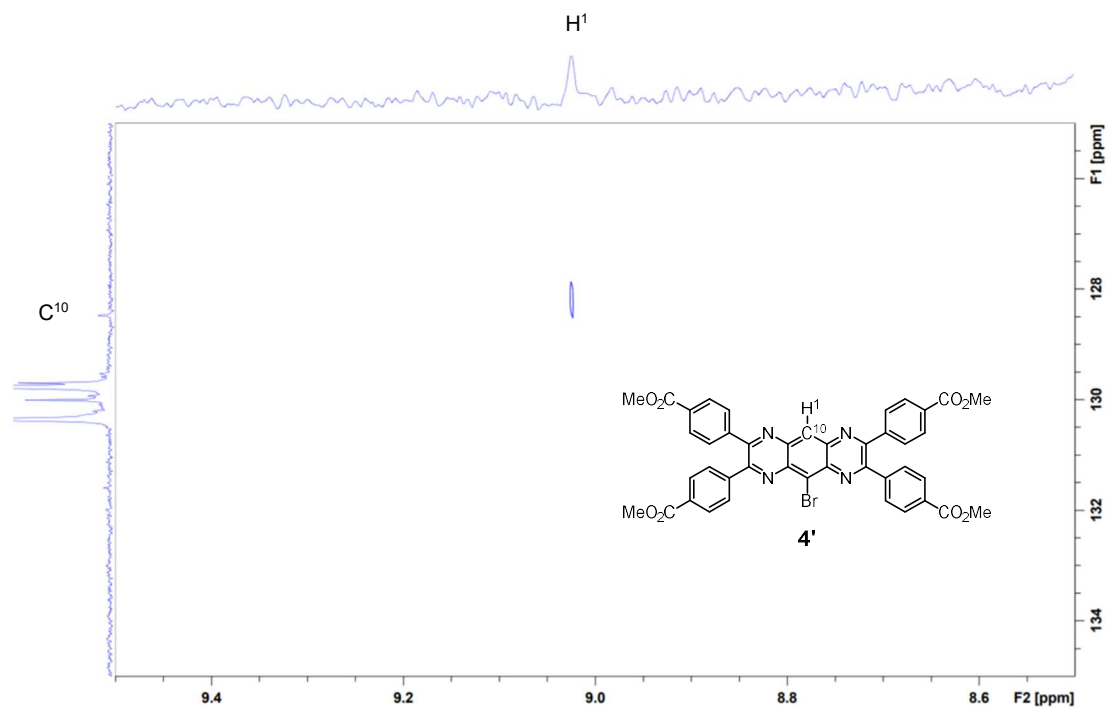


Fig. S14 ^1H -detected multiple quantum coherence (HMQC) (100 MHz, CDCl_3) spectrum of a mixture of **4** and **4'**. A cross peak is observed between H^1 and C^{10} , indicating formation of **4'**.

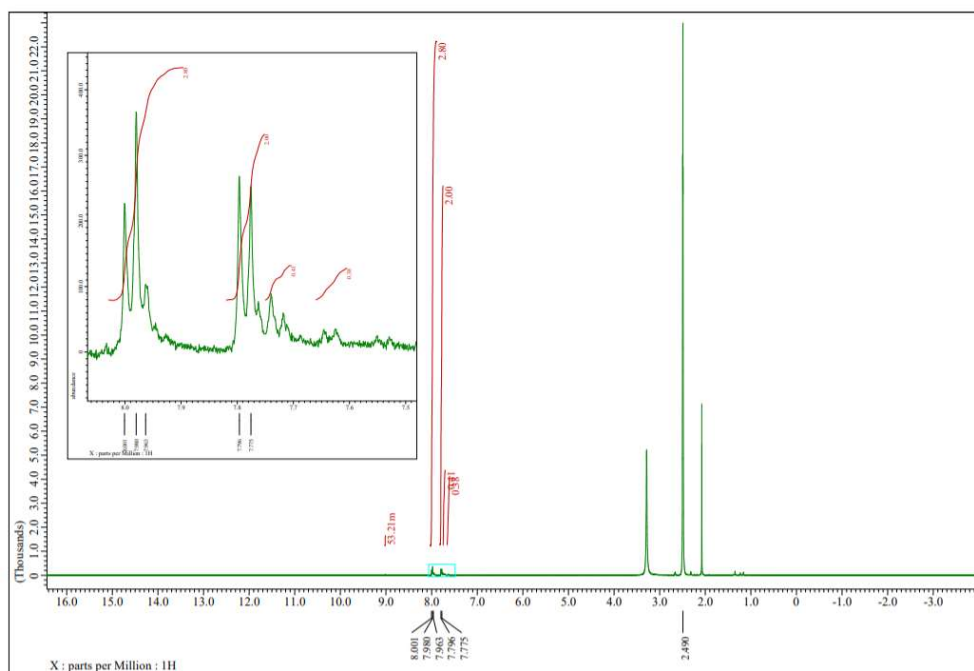


Fig. S15 ^1H NMR (400 MHz, $\text{DMSO-}d_6$) spectrum of a mixture of **BrPQ** and **Br(H)PQ**. A molar ratio of **BrPQ** : **Br(H)PQ** is 1 : 0.4.

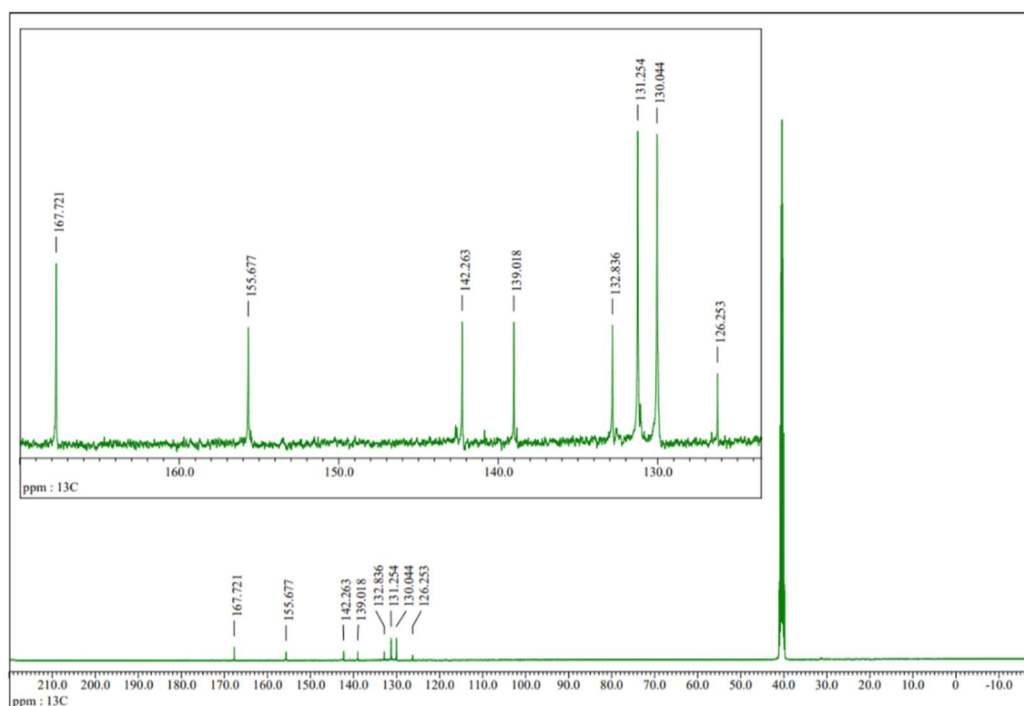


Fig. S16 ^{13}C NMR (100 MHz, $\text{DMSO-}d_6$) spectrum of **BrPQ** and **Br(H)PQ**. Only peaks of **BrPQ** are picked.

9. References

- S1. Rigaku Oxford Diffraction (2015), Software CrysAlisPro 1.171.38.41o. Rigaku Corporation, Tokyo, Japan.
- S2. G. M. Sheldrick, *Acta Crystallogr. Sect. A*, 2015, **71**, 3–8.
- S3. Rigaku (2018). CrystalStructure. Version 4.3. Rigaku Corporation, Tokyo, Japan. S4. G. M. Sheldrick, *Acta Crystallogr. C*, 2015, **71**, 3–8.
- S5. (a) P. v. d. Sluis and A. L. Spek, *Acta Crystallogr. Sect. A*, 1990, **46**, 194. (b) A. L. Spek, *Acta Crystallogr. Sect. D*, 2009, **65**, 148–155.
- S6. A. Schleper, C. Voll, J. Engelhart and T. Swager, *Synlett*, 2017, **28**, 2783–2789.